PHOTONICS Research

Lorentz-invariant space-time wave packets

VINZENZ ZIMMERMANN AND MIGUEL A. BANDRES*

CREOL – The College of Optics and Photonics, University of Central Florida, Orlando, Florida 32816, USA
**Corresponding author: bandres@creol.ucf.edu*

Received 15 May 2025; revised 25 August 2025; accepted 28 August 2025; posted 3 September 2025 (Doc. ID 567352); published 0 MONTH 0000

Non-diffractive space-time wave packets (nSTWPs) represent a broad class of optical pulses capable of propagating without diffraction or dispersion in linear media. In this work, we introduce a complete family of nSTWPs that remain invariant under transverse Lorentz boosts. The Lorentz-invariant behavior of these STWPs is rigorously analyzed through their associated spectral line function, providing new insights into their fundamental properties. Furthermore, we quantify the limitations of this invariance and compare the robustness of the proposed nSTWPs against conventional nSTWPs. These findings highlight the potential of Lorentz-invariant nSTWPs for applications in robust wave packet design and space-based optical communications.

https://doi.org/10.1364/PR.567352

1. INTRODUCTION

Analytical solutions to the Helmholtz wave equation play a fundamental role in optics, not only because they provide a rigorous framework for describing and analyzing optical fields but, more importantly, because they are intrinsically tied to symmetries—and, thus, to conserved physical quantities—that render their propagation unique. The best-known example is beams carrying optical angular momentum (OAM), where, due to rotational symmetry, their OAM is conserved and quantized [1]. Another important subset of structured light is non-diffractive beams [2–4], that can, in theory, propagate without experiencing diffraction due to the conservation of their propagation momentum k_z. This conservation of momentum also imposes that the transverse profile of the beam carries infinite energy, just as a plane wave. However, finite versions of such beams still possess a quasi-non-diffractive behavior in a finite conical region of space, making them extremely useful for several applications. In this way, thanks to the unique propagation properties of structured light [5] arising from the underlying symmetries and conserved quantities, structured light has found a plethora of applications in communication [6], optical trapping and manipulation [7], fabrication [8], microscopy and imaging [9,10], and quantum technologies [11], among many others [12].

Recently, the field of structured light underwent a broader development by moving from monochromatic CW structured beams to structured space-time wave packets (STWPs). Certain realizations of STWPs, namely focus wave modes [13] and X-waves [14], have been known for decades. However, interest in this area has surged following the recent introduction of non-diffractive space-time wave packets (nSTWPs) [15–17]. Counterintuitively, nSTWPs exhibit a spatio–temporal field that propagates without diffraction or dispersion in linear media. As it is common in structured light, these pulses exhibit discontinuities that prevent perfect physical realizations. In this case, their spectrum involves a delta function that constrains the longitudinal momentum k_z to a specific value, while enforcing the dispersion relation through a parabolic relationship between the transverse momentum k_x and the frequency ω [16]. Nonetheless, it has been demonstrated that nSTWPs can still be experimentally realized in a manner that preserves their non-diffractive and dispersionless behavior over a finite, yet practically significant, propagation distance. When measured in terms of the Rayleigh length z_R of Gaussian beams with the same spatial bandwidth, their non-diffractive propagation has been observed to extend over distances orders of magnitude larger than z_R [18,19].

These unique properties of nSTWPs have stimulated the development of advanced schemes for manipulating spatio–temporal fields, enabling their efficient generation [20–24] for practical applications. These developments have opened the door to exploring other intriguing features of nSTWPs, such as self-healing [25], propagation at arbitrary group velocities [26], anomalous refraction [27], controllable departures from non-diffractive behavior [28], and orbital angular momentum [17], as well as nSTWPs in waveguiding structures [29,30] and non-diffractive wave packets at the single-photon level [31]. The idea of studying nSTWPs in reference frames connected by longitudinal Lorentz boosts has led to the discovery of ultrashort tilted-pulse-front nSTWPs [32] and has been proven to be experimentally viable [33].

In this work, we introduce a complete family of nSTWPs that remains invariant under transverse Lorentz boosts. In other words, observers moving at any transverse velocity relative to the wave packet will detect an identical spatio–temporal field. By studying the action of transverse Lorentz boosts in the spectral domain, we identify the unique class of nSTWPs that exhibits true Lorentz invariance. We characterize these wave packets through their spectral representation in frequency space and via an analytical closed-form solution in space-time. We rigorously examine their Lorentz-invariant behavior in both representations, uncovering fundamental properties that distinguish them from conventional STWPs. Furthermore, we propose a physical realization of these pulses and quantify their robustness under transverse boosts in comparison with conventional wave packets. These findings highlight the potential of Lorentz-invariant STWPs for applications in robust wave packet design, atomic optics, and space-based optical communications.

2. SPECTRAL REPRESENTATION OF LORENTZ-INVARIANT nSTWPs

We start by considering the 2D scalar wave equation, $(\partial_x^2 + \partial_z^2 - \partial_t^2/c^2)\Psi(x,z,t) = 0$. In Refs. [15,16], it was shown that a broad class of optical wave packets capable of propagating without diffraction or dispersion in linear media (nSTWPs) can be described by

$$\Psi(x,z,t) = e^{ik_L z} \int A(\eta) e^{ik_L (x \sinh \eta - ct \cosh \eta)} \mathrm{d}\eta. \tag{1}$$

This formulation defines a one-to-one mapping between the spectral line function $A(\eta)$ and the corresponding nSTWP. By tailoring the spectral line function $A(\eta)$, a wide variety of distinct nSTWPs can be realized. Note that the solution is separable in z; hence, the evolution of the wave packet reduces to the pure accumulation of a global phase:

$$\Psi(x,z,t) = e^{ik_L z}\Psi(x,0,t) = e^{ik_L z}\psi(x,t). \tag{2}$$

As a result, the intensity profile becomes propagation-invariant, $I(x,z,t) = I(x,t)$, indicating that the wave packet propagates without diffraction or dispersion.

Analyzing the problem directly at the level of the wave equation provides a complementary viewpoint to the spectral representation described above. To do this, we substitute the separable ansatz $\Psi(x,z,t) = e^{ik_L z}\psi(x,t)$ into the original 2D scalar wave equation. This substitution simplifies the problem, reducing it directly to the modified wave equation $(\partial_x^2 - \partial_t^2/c^2 - k_L^2)\psi(x,t) = 0$. This equation is mathematically identical to the $(1+1)$-dimensional Klein–Gordon equation. The spatio–temporal pulse envelope $\psi(x,t)$ plays the role of the scalar field describing a spinless relativistic quantum particle of mass m, while the longitudinal propagation constant k_L corresponds directly to the effective mass term $mc/\hbar$. This approach, thus, clearly reveals the fundamental analogy between these optical wave packets and relativistic wave dynamics.

Let us now consider the action of Lorentz transformations on nSTWPs. In $(1+1)$-dimensional Minkowski space-time, a transversal Lorentz transformation corresponds to a Lorentz boost along the x-axis with velocity v. Under this boost, the space-time coordinates (t,x) in the original reference frame transform to the boosted reference frame (t',x') according to $ct' = ct\cosh\theta - x\sinh\theta, x' = x\cosh\theta - ct\sinh\theta$, where $\theta = \tanh^{-1}(v/c)$ is the rapidity. The boosted nSTWP, $\Psi_\theta(x',t')$, is obtained by evaluating the original wave packet at the event that corresponds to (x',t') in the rest frame, i.e., $\Psi_\theta(x',t') = \Psi(x(x',t'),t(x',t'))$. More importantly, the boosted wave packet can also be computed directly in the spectral representation by using Eq. (1) [34]; see Appendix A. In frequency space, we find that a Lorentz boost corresponds to a simple translation of the spectral line function, that is, $A^\theta(\eta) = A(\eta+\theta)$.

An nSTWP that is invariant under a Lorentz boost must look exactly the same as the original nSTWP, up to a global phase; that is, $\Psi_\theta(x',t') = \Psi(x',t')e^{i\phi}$. At the level of the spectral line function, this invariance condition implies that $A^\theta(\eta) = A(\eta)e^{i\phi}$ and, therefore, constrains the spectral line function to be translation-invariant. The only function satisfying this condition is the complex exponential function. Therefore, the first main result of this work is that the spectral line function of a Lorentz-invariant nSTWP must have the following form:

$$A_\zeta(\eta) = e^{i\zeta\eta}, \tag{3}$$

where ζ is a real parameter that uniquely characterizes each Lorentz-invariant nSTWP. Additionally, nSTWPs corresponding to different values of ζ are orthogonal to each other; this is demonstrated by evaluating the inner product between two fields in frequency space. The special case of $\zeta = 0$ corresponds to a constant spectral amplitude, $A(\eta) = 1$, which was one of the first nSTWPs proposed in Refs. [15,16]; however, Lorentz invariance was not discussed at all in those studies. The experimental realization of these Lorentz-invariant nSTWPs can be achieved via spatiotemporal Fourier synthesis using a spatial light modulator, as described in Refs. [18–21,33], by implementing the spectral line function defined in Eq. (3).

3. SPACE-TIME REPRESENTATION OF LORENTZ-INVARIANT nSTWPs

Now that we have the general spectral representation of the Lorentz-invariant nSTWP, we will find its representation in space-time. By evaluating Eq. (1) using the spectral line function in Eq. (3), we find that the Lorentz-invariant nSTWPs are given by

$$\psi_\zeta(u,v) = K_{i\zeta}(ik_L u)e^{i\zeta v}, \tag{4}$$

where $K_{i\zeta}$ is the modified Bessel function of the second kind of complex order $i\zeta$, and (u,v) are the hyperbolic coordinates defined by the transformation $t = u\cosh v$, $x = u\sinh v$. The coordinate $u^2 = t^2 - x^2$ represents the proper time, or hyperbolic radius, from the origin to the event (t,x), hence, lines of constant u trace hyperbolae. The coordinate v, known as the rapidity, determines the velocity of an inertial observer who passes through both the origin and the point (t,x). Each value of v corresponds to a constant velocity given by $\tanh v = x/t$, with lines of constant v forming straight lines through the origin; see Appendix B. To describe the spacelike region where $t^2 - x^2 < 0$, the standard approach in the literature is to introduce a separate coordinate system altogether. However, we have found it more convenient to *promote* (u,v) to complex

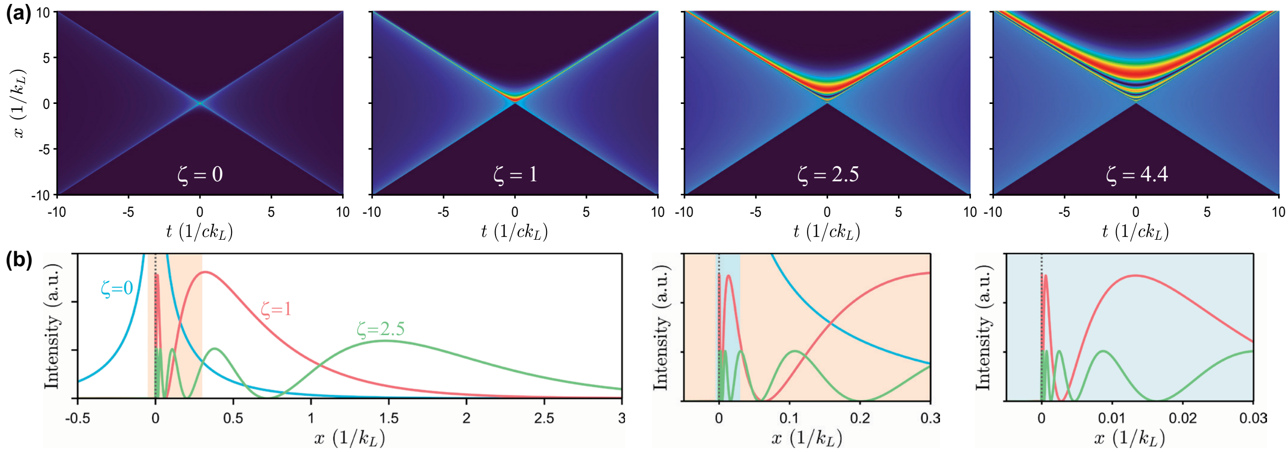

Fig. 1. *Lorentz-invariant space-time wave packets.* (a) Propagation dynamics of Lorentz-invariant pulses for various values of ζ. (b) Corresponding transverse cross-sections at $t = 0$. The right-hand plot is a zoomed-in view of the shaded region around $x = 0$. As ζ increases, additional intensity lobes emerge along $x > 0$. Pulses with $\zeta < 0$ are mirror reflections across the x-axis of those with $\zeta > 0$. Each pulse is independently normalized and saturated for better visualization.

coordinates in order to cover all of Minkowski space-time in a unified manner. For example, choosing $u = i\rho$ and $v = w + i\pi/2$ ($\rho, w \in \mathbb{R}$) extends coverage to the entire region *outside* the light cone ($t^2 - x^2 < 0$). In this way, the combined real and complex patches together cover all of (1 + 1)-dimensional space-time. As expected, the solution in Eq. (4) falls within the class of analytic solutions to the (1 + 1)-dimensional Klein–Gordon equation [35].

In Fig. 1, we show the space-time intensity field distribution for several Lorentz-invariant nSTWPs with different values of the order parameter ζ. As ζ increases, the initial intensity peak shifts along x, and additional intensity lobes emerge from the origin, as illustrated in Fig. 1. Wave packets with $\zeta < 0$ are mirror reflections across the x-axis of those with $\zeta > 0$. From Eq. (4), we see that the parameter k_L acts as a purely axial scaling factor, stretching the field distribution along the u-coordinate. Demonstrating the Lorentz invariance of these wave packets in their space-time representation becomes straightforward using the hyperbolic coordinates (u, v). Under a Lorentz boost with rapidity θ, the coordinates transform as $(u', v') = (u, v - \theta)$. Therefore, the boosted field is generally given by $\psi_\theta(u', v') = \psi_0(u, v) = \psi_0(u', v' + \theta)$. Applying this relation to our Lorentz-invariant wave packets in Eq. (4), we obtain $\psi_{\theta,\zeta}(u', v') = \psi_{0,\zeta}(u', v')e^{i\zeta\theta}$, confirming that the wave packet remains invariant up to a global phase factor.

Notably, as shown in Fig. 2(b), the Lorentz-invariant nSTWP exhibits a branch-point singularity at the origin, $(t, x) = (0,0)$, which propagates as a discontinuity along the surface of the light cone. For $\zeta > 0$, the field at $t = 0$ is nonzero only for $x > 0$, giving rise to the observed discontinuity, where the field oscillates increasingly rapidly as it approaches $x = 0$. The origin of this singular behavior lies in the spectral line function, where all wavelengths contribute to the wave packet. For a physically realizable wave packet with finite energy and without discontinuities, the spectral line function $A(\eta)$ must be apodized. A simple and elegant way to introduce a smooth, analytic apodization is by applying a small imaginary shift to the time coordinate, $t \to t - iq$, as previously studied for general STWPs in Ref. [16]. In this way, the apodized line function becomes $A_q(\eta) = A(\eta)e^{-qck_L \cosh \eta}$, where the exponential term acts as a Gaussian-like apodization with strength parameter q. A key advantage of this approach is that the apodized version of the nSTWP in space-time can be obtained by simply replacing the time variable with a complex shift, $t \to t - iq$, in the analytic solution given in Eq. (4). The effects

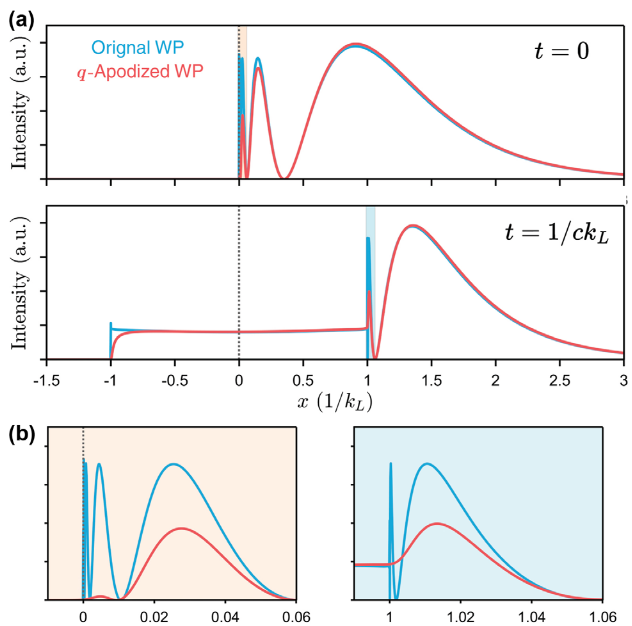

Fig. 2. *q-apodized Lorentz-invariant space-time wave packets.* (a) Intensity distribution of a Lorentz-invariant nSTWP (blue) with $\zeta = 1.8$ and its q-apodized version (red) for $q = 5 \times 10^{-3}$, shown at times $t = 0$ and $t = 1/(ck_L)$. (b) Insets at the bottom highlight the singularity regions at the light cone, marked in orange and blue in the main panels. While the ideal Lorentz-invariant nSTWP exhibits a singularity, the q-apodized version remains smooth.

of this apodization are illustrated in Fig. 2, where it is evident that the field discontinuity near the light cone disappears as the apodization parameter q is introduced.

Although apodizing the infinite spectral line function in Eq. (3) eliminates the branch-point singularity present in an ideal Lorentz-invariant nSTWP, it also breaks the translational invariance of the spectrum and, consequently, its exact Lorentz invariance. Nevertheless, if the apodization is sufficiently weak, the resulting wave packet retains a high degree of quasi-Lorentz invariance under transverse boost—that is, no qualitative changes in the shape of the pulse are observed. We understand the wave packet to be quasi-invariant when the overlap remains near unity over the entire range of considered boosts, $\mathcal{O}(v) > 0.95$. To illustrate this behavior, we present two apodized Lorentz-invariant nSTWPs and one generic nSTWP in Fig. 3. We construct the apodized wave packets using two methods: a super-Gaussian apodization [Fig. 3(a)] and a q-parameter-based apodization [Fig. 3(b)]. Given a fixed bandwidth for the spectral line function, the super-Gaussian profile is near-optimal among physically realizable apodization strategies: it effectively approximates a flat-top profile, while its smooth edges suppress the oscillatory artifacts introduced by abrupt truncations. The generic wave packet [Fig. 3(c)] is obtained by taking only the real part of the field in Fig. 3(b), which strongly breaks the translational invariance of the spectral line function. In the middle row of Fig. 3, we show the space-time intensity profiles for all three wave packets, both in the rest frame and in a transversely boosted frame with velocity $v = 0.6c$. The apodized Lorentz-invariant wave packets in Figs. 3(a) and 3(b) exhibit only minor deviations under the boost, while the generic wave packet in Fig. 3(c) shows substantial distortion and a pronounced skew in the space-time field structure.

To visualize Lorentz invariance more clearly, we show in the last column of Fig. 3 the transverse intensity cross-sections at $t = 1/(ck_L)$ for the Lorentz-invariant nSTWPs and the generic nSTWP for various transverse boost velocities up to $v = 0.6c$. The deviations of the apodized Lorentz-invariant wave packets are minimal and are most visible in the zoomed-in inset at the intensity peak located at $x = -1$. Similar behavior is observed at the peak at $x = +1$, but with the opposite trend: its height increases gradually with increasing boost velocity, while its width remains nearly unchanged. In contrast, the deviations of the generic wave packet under transverse boosts are clearly visible and significantly more pronounced.

Furthermore, to quantify the Lorentz invariance of the wave packets, we calculate the overlap integral between the field in the rest frame and its counterpart in the boosted frame as a function of the transverse boost velocity:

$$\mathcal{O}(v) = \left| \int (\partial_t \Psi^*_{v=0}(x,t))\Psi_v(x,t)\mathrm{d}x \right|; \quad \text{(5)}$$

at any constant time t. Interestingly, for nSTWPs represented through the spectral formulation in Eq. (1), this overlap can be more conveniently computed in the spectral domain using the spectral line functions,

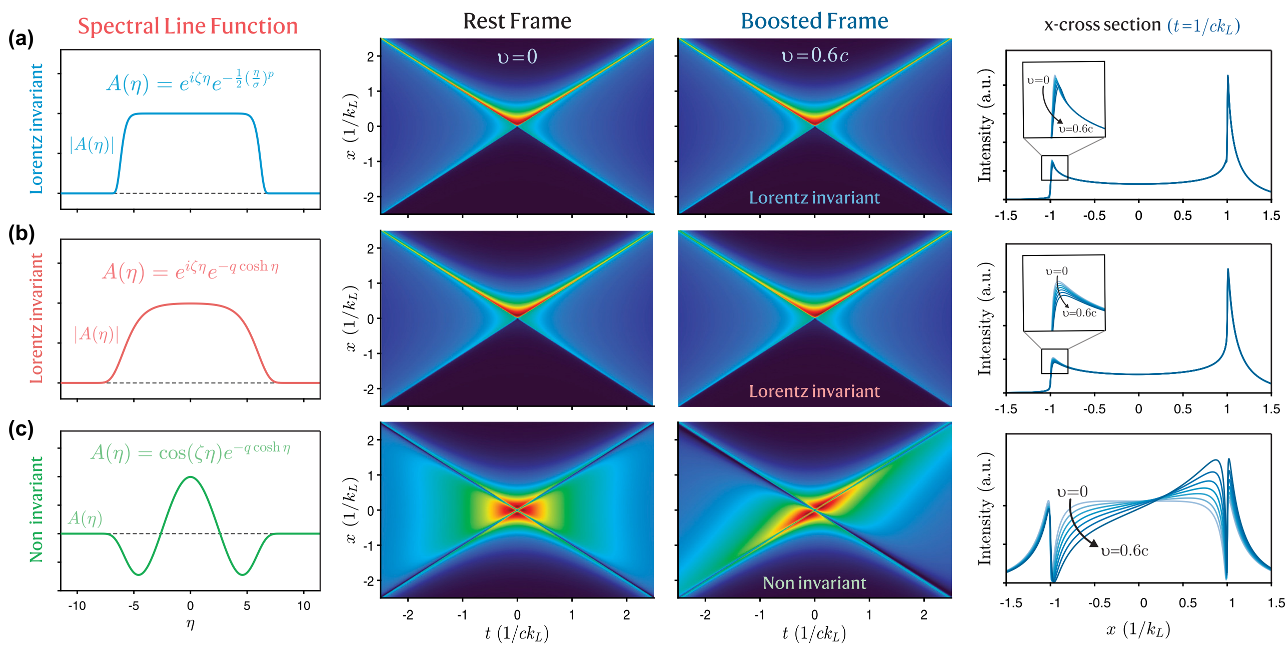

Fig. 3. *Transverse boost invariance of apodized Lorentz-invariant nSTWPs.* (a), (b) Spectral line function (left column) and intensity profiles of the wave packet in the rest frame and in a transversely boosted frame (center columns), for a super-Gaussian apodization ($\sigma = 6, p = 20$) in (a) and a q-apodized ($q = 5 \times 10^{-3}$) Lorentz-invariant nSTWP in (b), both with $\zeta = 0.6$. (c) Same as (a), (b), but for a non-invariant nSTWP. The apodized Lorentz-invariant wave packets in (a) and (b) remain largely unchanged under the transverse boost, while the non-invariant wave packet in (c) is visibly distorted. Transverse intensity cross-sections (right column) at $t = 1/(ck_L)$ for various transverse boost velocities, comparing the robustness of the Lorentz-invariant nSTWP (a), (b) against the generic nSTWP (c). The results highlight the superior resilience of Lorentz-invariant wave packets.

$$\mathcal{O}(v) = \left| \int A^*_{v=0}(\eta) A_v(\eta) \mathrm{d}\eta \right|; \quad \textbf{(6)}$$

see Appendix C. This representation not only simplifies numerical evaluation but also provides direct insight into how Lorentz invariance emerges from the shift properties of the spectral line function. Using this overlap integral, Fig. 4(a) quantifies the transverse boost invariance of the q-apodized quasi-Lorentz-invariant and the generic nSTWPs shown in Fig. 3(a) and 3(c), respectively. We clearly see that the q-apodized Lorentz-invariant wave packet remains nearly unchanged under transverse boosts up to $v = 0.9c$, maintaining an overlap of 0.95 with its rest-frame counterpart. In contrast, the generic wave packet deviates noticeably even at moderate boost velocities, with the overlap dropping to 0.563 at $v = 0.9c$. We examine this behavior further in Figs. 4(b) and 4(c), which show the overlap integrals not only as a function of transverse boost velocity but also across a range of apodization parameters, $q \in [1 \times 10^{-5}, 1]$. As expected, for the q-apodized Lorentz-invariant wave packet [Fig. 4(b)], variations in the overlap arise primarily from the increase in the apodization parameter q, which is responsible for breaking exact Lorentz invariance. At small values of q, the overlap remains close to unity even for boost velocities approaching $v = c$. For the generic nSTWP [Fig. 4(c)], the significant decrease of the overlap with increasing boost velocity is mostly independent of q. This behavior arises from the inherent lack of shift invariance in the underlying spectral line function. Note that, due to the periodicity of the $\cos(\zeta\eta)$ modulation used in our example of a generic nSTWP, a high degree of boost invariance may be recovered at certain velocities when the modulation frequency ζ is sufficiently large; see Fig. 4(a) as $v \to c$. This effect is an artifact of choosing a periodic spectral line function for the generic wave packet and does not reflect true Lorentz invariance. Overall, these results confirm that Lorentz-invariant fields, even when mildly apodized, offer a uniquely robust platform for preserving the space-time field structure under relativistic transverse boosts.

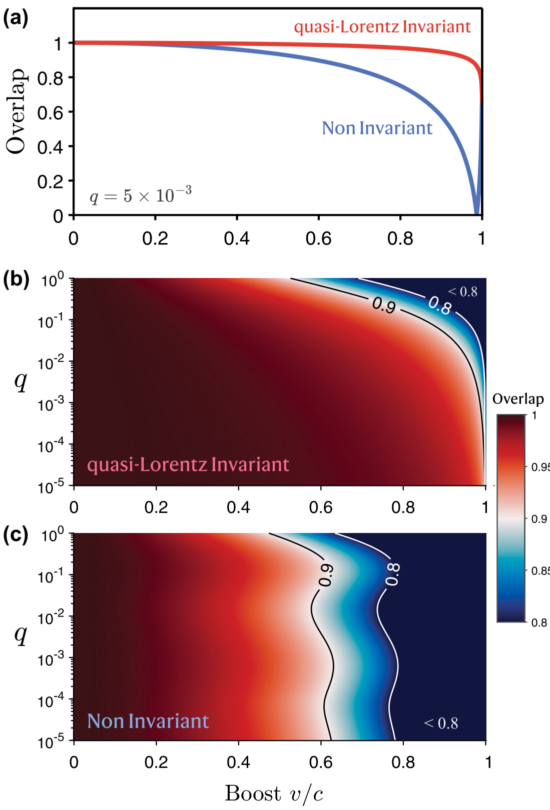

Fig. 4. *Quantifying transverse boost invariance* of a q-apodized quasi-Lorentz-invariant and a generic nSTWP. (a) Overlap between each wave packet in the rest frame and its transversely boosted counterpart as a function of boost velocity v, for $q = 5 \times 10^{-3}$ and $\zeta = 0.6$. (b), (c) Overlap evaluated over a range of apodization strengths q for the quasi-Lorentz-invariant wave packet (b) and the generic wave packet (c). In (b), the overlap remains near unity and is remarkably stable across all boost velocities, confirming the strong quasi-Lorentz invariance of the q-apodized wave packet; in contrast, (c) shows a pronounced decay with increasing v, revealing the sensitivity of the generic wave packet to transverse boosts.

4. CONCLUSION

In conclusion, we have introduced and analyzed a complete family of space-time wave packets that are invariant under transverse Lorentz boosts. By identifying the precise spectral condition for Lorentz invariance, we derived a unique class of non-diffractive, non-dispersive wave packets characterized by a one-parameter family of spectral line functions. Additionally, we obtained analytic, closed-form expressions that describe these wave packets directly in space-time. Our analysis revealed that ideal Lorentz-invariant STWPs exhibit a singularity at the light cone, which we mitigated using a smooth analytic apodization. Remarkably, we showed that the apodized wave packets still retain a high degree of Lorentz invariance under transverse boosts. This quasi-invariant behavior clearly sets them apart from generic nSTWPs and highlights their exceptional robustness. Altogether, our findings deepen the theoretical understanding of space-time wave packet symmetries and pave the way for the design of resilient optical pulses. Lorentz-invariant wave packets hold strong potential for applications in space-based optical communication, atomic optics, and robust information encoding in dynamic environments.

APPENDIX A: SPECTRAL SPACE REPRESENTATION OF LORENTZ BOOSTS

The action of a transverse Lorentz boost in spectral space is determined by evaluating the spectral line integral in the boosted reference frame,

$$\begin{aligned}
\Psi_\theta(x',t') &= \Psi(x(x',t'),t(x',t')) \\
&= \int \mathrm{d}\eta A(\eta) e^{ik_L(x(x',t')\sinh\eta - ct'(x',t')\cosh\eta)} \\
&= \int \mathrm{d}\eta A(\eta) e^{ik_L[(x'\cosh\theta + ct'\sinh\theta)\sinh\eta - (ct'\cosh\theta + x'\sinh\theta)\cosh\eta]} \\
&= \int \mathrm{d}\eta A(\eta) e^{ik_L(x'\sinh(\eta-\theta) - ct'\cosh(\eta-\theta))} \\
&= \int \mathrm{d}\tilde{\eta} A(\tilde{\eta}+\theta) e^{ik_L(x'\sinh\tilde{\eta} - ct'\cosh\tilde{\eta})}. \quad \textbf{(A1)}
\end{aligned}$$

Therefore, we conclude that a transverse Lorentz boost acts on nSTWPs by translating their associated line function in spectral space, such that $A^{\theta}(\eta) = A(\eta + \theta)$.

APPENDIX B: HYPERBOLIC COORDINATES AND LORENTZ INVARIANCE

While it is convenient to work in spectral space, the inherent boost invariance of the Lorentz nSTWPs can also be recognized in space-time through their associated hyperbolic coordinates, sketched in Fig. 5(a). The hyperbolic radius $u^2 = t^2 - x^2$ corresponds precisely to the definition of the space-time metric $\sigma^2 = t^2 - x^2$, which is known to remain invariant under Lorentz transformations between inertial reference frames. We conclude that the coordinate u does not change when transitioning from a rest frame to a boosted reference frame. Using the inversion $\tanh\, v = x/t$, it can be shown that v transforms according to $v' = v - \theta$. This implies that Lorentz nSTWPs are invariant up to a global phase, $\psi_{\theta,\zeta}(u', v') = \psi_{0,\zeta}(u', v')e^{i\zeta\theta}$. This is illustrated in Figs. 5(b) and 5(c), where we show the field distribution of the Lorentz-invariant wave packets as observed in a rest frame ($v = 0$) and in a boosted frame ($v = 0.6c$). Under a Lorentz boost, Cartesian coordinates undergo a shear transformation. In Fig. 5(b), this is illustrated by the dashed white lines, which represent the axes of the boosted frame as viewed from the rest frame. In contrast, Fig. 5(c) shows the same field as observed in the boosted frame, where the coordinate lines appear orthogonal. Despite this transformation, the shape of the pulse remains invariant, and the field acquires only a global phase.

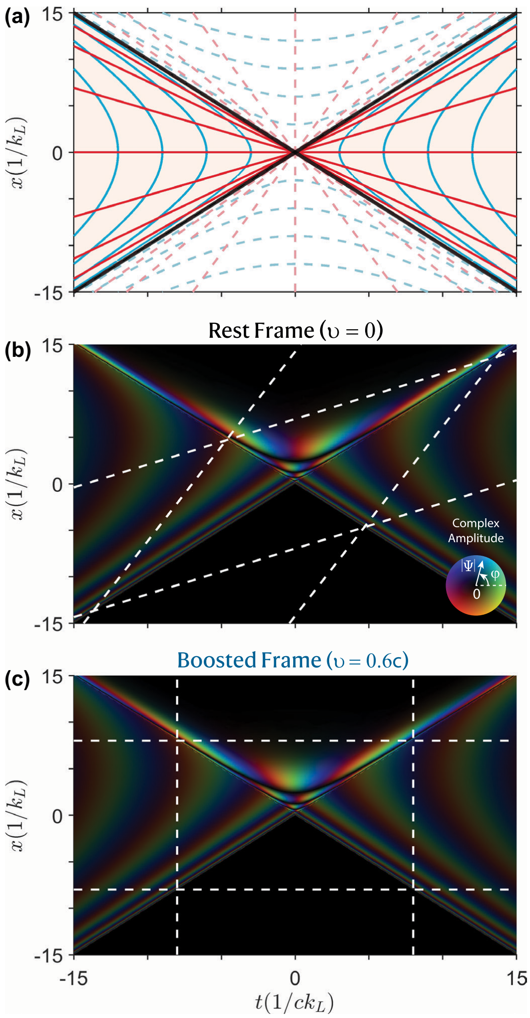

Fig. 5. *Hyperbolic coordinates and Lorentz-invariant wave packets in different reference inertial frames.* (a) Lines of constant u trace hyperbolas (solid blue), while lines of constant v are straight lines (solid red) passing through the origin of space-time. Outside the light cone, u and v become complex, but their constant-value contours still trace hyperbolas and lines through the origin, respectively (dashed lines). (b), (c) Space-time field distribution of the Lorentz-invariant wave packets ($\zeta = 5$) as observed in a rest frame ($v = 0$) and a boosted frame ($v = 0.6c$), respectively. In (b), the dashed white lines indicate the Cartesian axes of the boosted frame as embedded in the rest frame, where they appear skewed due to the Lorentz shear. In (c), the field is shown directly in the boosted frame, where the coordinate lines appear orthogonal. The Lorentz-invariant wave packet maintains its shape under the Lorentz transformation while acquiring only a global phase.

APPENDIX C: OVERLAPS IN SPECTRAL SPACE

To quantify the degree of robustness of nSTWPs against transverse Lorentz boosts, we evaluate the overlap $O(v)$ between the wave packets in the rest and boosted reference frames at a fixed time t_0, assuming the initial pulses are normalized. These overlaps are most conveniently evaluated directly from the spectral line functions using Eq. (5). The simplicity of this expression allows us to compute the overlap for the Lorentz-invariant wave packets in Eq. (4) exactly as

$$\mathcal{O}(v) = \left| \frac{K_0(2q\cosh(\theta/2))}{K_0(2q)} \right|, \tag{C1}$$

where $\theta = \tanh^{-1}(v/c)$ is the rapidity associated with the boost. This analytical result is shown in Fig. 4(b), and it agrees perfectly with the numerical evaluation. To define the overlaps in Eq. (5), we used the natural inner product associated with the wave equation, which involves integrating the product of one wave packet with the time derivative of the other. Interestingly, since we consider only positive-frequency solutions, the paraxial inner product, analogous to the standard L^2 inner product and defined without time derivatives, is also well defined and conserved in time. In this case, the inner product of a wave packet with itself remains constant during evolution. For this reason, we can also define the overlap using

$$\mathcal{O}_P(v) = \left| \int \mathrm{d}x \Psi^*_{v=0}(x,t)\Psi_v(x,t) \right|_{t=t_0} = \left| \int \mathrm{d}\eta \frac{A^*_{v=0}(\eta)A_v(\eta)}{k_L \cosh\eta} \right|. \tag{C2}$$

As shown in Fig. 6, the robust Lorentz invariance of the proposed wave packets in Eq. (4) remains unchanged when this more conventional definition of the inner product is adopted.

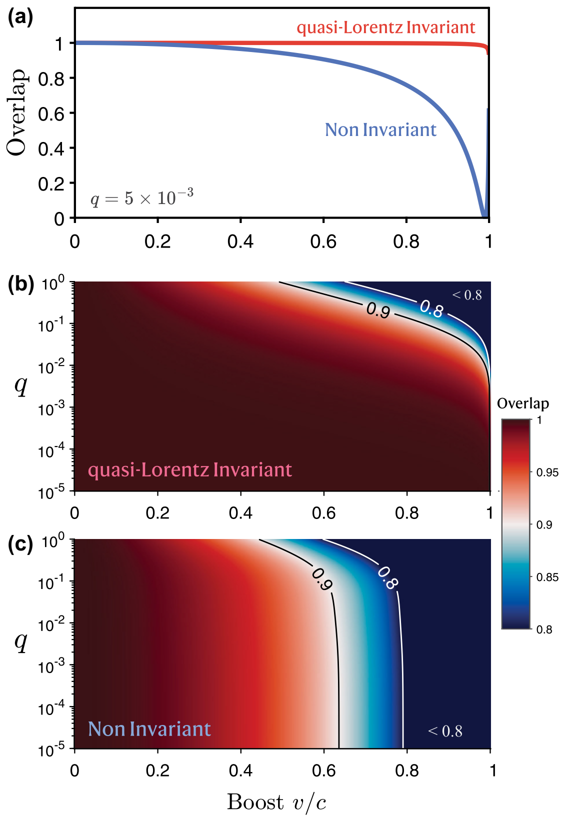

Fig. 6. *Quantifying transverse boost invariance using the standard L^2 inner product* of a q-apodized quasi-Lorentz-invariant and a generic nSTWP (usual definition of inner product). (a) Overlap between each wave packet in the rest frame and its transversely boosted counterpart as a function of boost velocity v, for $q = 5 \times 10^{-3}$ and $\zeta = 0.6$. (b), (c) Overlap evaluated over a range of apodization strengths q for the quasi-Lorentz-invariant wave packet (b) and the generic wave packet (c). In (b), the overlap remains near unity and is remarkably stable across all boost velocities, confirming the strong quasi-Lorentz invariance of the q-apodized wave packet; in contrast, (c) shows a pronounced decay with increasing v, revealing the sensitivity of the generic wave packet to transverse boosts.

Funding. National Science Foundation (2207964).

Acknowledgment. V. Z. thanks Konrad Tschernig for helpful discussions during the early stages of this project.

Disclosures. The authors declare no conflicts of interest.

Data Availability. All information needed to reproduce the results is present in the paper.

REFERENCES

1. A. M. Yao and M. J. Padgett, "Orbital angular momentum: origins, behavior and applications," Adv. Opt. Photonics **3**, 161–204 (2011).
2. J. Durnin, "Exact solutions for nondiffracting beams. I. The scalar theory," J. Opt. Soc. Am. A **4**, 651–654 (1987).
3. J. C. Gutiérrez-Vega, M. D. Iturbe-Castillo, and S. Chávez-Cerda, "Alternative formulation for invariant optical fields: Mathieu beams," Opt. Lett. **25**, 1493–1495 (2000).
4. M. A. Bandres, J. C. Gutiérrez-Vega, and S. Chávez-Cerda, "Parabolic nondiffracting optical wave fields," Opt. Lett. **29**, 44–46 (2004).
5. A. Forbes, M. De Oliveira, and M. R. Dennis, "Structured light," Nat. Photonics **15**, 253–262 (2021).
6. G. Gibson, J. Courtial, M. J. Padgett, *et al.*, "Free-space information transfer using light beams carrying orbital angular momentum," Opt. Express **12**, 5448–5456 (2004).
7. E. Otte and C. Denz, "Optical trapping gets structure: structured light for advanced optical manipulation," Appl. Phys. Rev. **7**, 041308 (2020).
8. D. Fan, L. Wang, and Y. Ekinci, "Nanolithography using Bessel beams of extreme ultraviolet wavelength," Sci. Rep. **6**, 31301 (2016).
9. T. A. Planchon, L. Gao, D. E. Milkie, *et al.*, "Rapid three-dimensional isotropic imaging of living cells using Bessel beam plane illumination," Nat. Methods **8**, 417–423 (2011).
10. T. Vettenburg, H. I. C. Dalgarno, J. Nylk, *et al.*, "Light-sheet microscopy using an Airy beam," Nat. Methods **11**, 541–544 (2014).
11. M. Mirhosseini, "High-dimensional quantum cryptography with twisted light," New J. Phys. **17**, 033033 (2015).
12. H. Rubinsztein-Dunlop, A. Forbes, M. V. Berry, *et al.*, "Roadmap on structured light," J. Opt. **19**, 013001 (2017).
13. J. N. Brittingham, "Focus waves modes in homogeneous Maxwell's equations: transverse electric mode," J. Appl. Phys. **54**, 1179–1189 (1983).
14. J.-Y. Lu and J. Greenleaf, "Nondiffracting X waves-exact solutions to free-space scalar wave equation and their finite aperture realizations," IEEE Trans. Ultrason. Ferroelectr. Freq. Control **39**, 19–31 (1992).
15. H. E. Kondakci and A. F. Abouraddy, "Diffraction-free pulsed optical beams via space-time correlations," Opt. Express **24**, 28659–28668 (2016).
16. K. J. Parker and M. A. Alonso, "Longitudinal iso-phase condition and needle pulses," Opt. Express **24**, 28669–28677 (2016).
17. M. Yessenov, L. A. Hall, K. L. Schepler, *et al.*, "Space-time wave packets," Adv. Opt. Photonics **14**, 455–570 (2022).
18. B. Bhaduri, M. Yessenov, and A. F. Abouraddy, "Meters-long propagation of diffraction-free space-time light-sheets," Opt. Express **26**, 20111–20121 (2018).
19. B. Bhaduri, M. Yessenov, D. Reyes, *et al.*, "Broadband space-time wave packets propagating 70 m," Opt. Lett. **44**, 2073–2076 (2019).
20. H. E. Kondakci and A. F. Abouraddy, "Diffraction-free space–time light sheets," Nat. Photonics **11**, 733–740 (2017).
21. A. Shiri, M. Yessenov, S. Webster, *et al.*, "Hybrid guided space-time optical modes in unpatterned films," Nat. Commun. **11**, 6273 (2020).
22. Y. J. Tan, P. Pitchappa, N. Wang, *et al.*, "Space-time wave packets from Smith-Purcell radiation," Adv. Sci. **8**, 2100925 (2021).
23. C. Guo, M. Xiao, M. Orenstein, *et al.*, "Structured 3D linear space–time light bullets by nonlocal nanophotonics," Light Sci. Appl. **10**, 160 (2021).
24. X. Su, K. Zou, Y. Wang, *et al.*, "Space-time wave packets in multimode optical fibers with controlled dynamic motions and tunable group velocities," Nat. Commun. **16**, 2027 (2025).
25. H. E. Kondakci and A. F. Abouraddy, "Self-healing of space-time light sheets," Opt. Lett. **43**, 3830–3833 (2018).
26. M. Yessenov and A. F. Abouraddy, "Accelerating and decelerating space-time optical wave packets in free space," Phys. Rev. Lett. **125**, 233901 (2020).
27. B. Bhaduri, M. Yessenov, and A. F. Abouraddy, "Anomalous refraction of optical spacetime wave packets," Nat. Photonics **14**, 416–421 (2020).
28. L. J. Wong, D. N. Christodoulides, and I. Kaminer, "The complex charge paradigm: a new approach for designing electromagnetic wave packets," Adv. Sci. **7**, 1903377 (2020).
29. B. Kibler and P. Béjot, "Discretized conical waves in multimode optical fibers," Phys. Rev. Lett. **126**, 023902 (2021).

30. C. Guo and S. Fan, "Generation of guided space-time wave packets using multilevel indirect photonic transitions in integrated photonics," Phys. Rev. Res. **3**, 033161 (2021).
31. J. Wang, Y. Zuo, X. Wang, *et al.*, "Spatiotemporal single-photon Airy bullets," Phys. Rev. Lett. **132**, 143601 (2024).
32. L. J. Wong and I. Kaminer, "Ultrashort tilted-pulse-front pulses and nonparaxial tilted-phase-front beams," ACS Photonics **4**, 2257–2264 (2017).
33. M. Yessenov, M. Romer, N. Ichiji, *et al.*, "Experimental realization of Lorentz boosts of space-time wave packets," Phys. Rev. A **109**, 013509 (2024).
34. E. G. Kalnins and W. Miller, Jr., "Lie theory and separation of variables. 3. The equation $f_{tt}–f_{ss} = \gamma^2 f$," J. Math. Phys. **15**, 1025–1032 (1974).
35. E. Kalnins, "On the separation of variables for the Laplace equation $\delta\psi + k^2\psi = 0$ in two- and three-dimensional Minkowski space," SIAM J. Math. Anal. **6**, 340–374 (1975).

Query

1. AU: The funding information for this article has been generated using the information you provided at the time of article submission. Please check it carefully. If any information needs to be corrected or added, please provide the full name of the funding organization/institution as provided in the CrossRef Open Funder Registry (https://search.crossref.org/funding).